Segmentation of brain MR images: a self-adaptive online vector quantization approach

Lihong Li [*a, b], Dongqing Chen [b], Hongbing Lu [b], and Zhengrong Liang [b, c]
Departments of Electrical & Computer Engineering [a], Radiology [b], and Computer Science [c]
State University of New York at Stony Brook, Stony Brook, NY 11794

ABSTRACT

We present a fully automatic algorithm for brain magnetic resonance (MR) image segmentation. The three-dimensional (3D) volumetric MR dataset is first interpolated for an adequate local intensity vector on each voxel. Then a morphology dilation filter and region growing technique are applied to extract the region of brain volume, strapping away the skull, scalp and other tissues. The principal component analysis (PCA) is utilized to generate a series of feature vectors from the local vectors via the Karhunen-Loéve (K-L) transformation for those voxels within the extracted region. We choose those first few principal components that sum up to, at least, 90% percent of the total variance for optimizing the dimensions of the feature vectors. Then a modified self-adaptive online vector quantization algorithm is applied to these feature vectors for classification. The presented algorithm requires no prior knowledge of the data distribution except a maximum number of distinct groups for classification, which can be set based on anatomical knowledge. Numerical analysis of the algorithm and experimental tests on brain MR images are presented. Results demonstrate efficient, robust, and self-adaptive properties of the presented algorithm.

Keywords: magnetic resonance image, image segmentation, feature extraction, Karhunen-Loéve transformation, self-adaptive vector quantization, computing efficiency.

1. INTRODUCTION

MR imaging technique has been widely used in studies of neural disorders. To facilitate diagnosis and therapy, tissue classification and segmentation are the key prerequisites toward quantifying the shape and volume of different types of tissues, which are then utilized for 3D visualization and feature analysis.

1.1. Review of MR image properties and previous work

In general, due to the technical limitations during image acquisition, MR images possess the following characteristics: (1) partial volume effect, (2) low spatial resolution, (3) non-uniformity effect induced by radio- frequency (RF) fields, and (4) high image contrast [3]. The review article [7] has described a number of MR image segmentation methods, which can be divided into two categories, supervised and unsupervised methods. Supervised techniques are knowledge-based methods, which require significant operator interaction and training [6,15]. Whereas unsupervised methods automatically find the tissue structures from the data [1,2,11,14,16]. In clinical application, one of the major obstacles for visualization is the difficulty in automating the segmentation.

Unsupervised techniques, also called cluster analyses, do not need user interaction or *a prior* knowledge of class structures. These approaches usually assume a model for intensity distributions of each class and then estimate the model parameters by fitting the images to the model [1,14,16]. The estimation can be very difficult and often requires long computation times. Other unsupervised methods applied in MR segmentation are the k-means [9] and the fuzzy c-means [2,11]. These methods succeed in classification of tumor volume, but rely on the initial value setup. A good initialization also helps to reduce the computation times. The well-known cluster analysis method for quantization, called Linde-Buzo-Gray (LBG) algorithm, has been widely used for the design of quantizer [10]. It minimizes the mean squared error and guarantees to converge to the local optimality. However, the following properties of LBG algorithm limit its application in MR segmentation: (1) it depends on the initial conditions, and (2) it requires an iterative procedure and long computation times.

[*]Correspondence: lli@clio.rad.sunysb.edu; Phone: 631-444-2508; Fax: 631-444-6450; http://clio.rad.sunysb.edu/micl; Laboratory for Imaging Research and Informatics, Department of Radiology, State University of New York, Stony Brook, NY 11794.

1.2. Outline of our method

In this paper, we focus on developing a self-adaptive clustering algorithm to achieve robust and efficient performance. Since cluster analysis method does not always converge to anatomical tissues [7], our method will integrate both intensity information and anatomy knowledge. The outline of our method is as follows.

An interpolation is first performed for an adequate local intensity vector on each voxel. This interpolation can mitigate the partial volume effect, while preserving the image contrast. In our study, we choose the first- and second-order neighbors for the local intensity vectors of 19 elements or dimensions. In order to extract the region of brain volume, a morphology dilation filter and region growing technique are applied [17]. The PCA is utilized in our method to generate the feature vectors via the K-L transformation. The first few principal components that sum up, at least, 90% percent of the total variance are chosen for optimizing the dimensions of the feature vectors. Then a modified self-adaptive online vector quantization algorithm (to be detailed below) is applied to these feature vectors for classification, which is self-adaptive to the data. The maximum number of classes for classification is preset based on the anatomical knowledge. After classification, the segmentation results will follow an inverse interpolation procedure and be resized back to the original image size.

The performance of our segmentation method was evaluated in three aspects using the anatomical model in the Connell Brain Imaging Center database of McGill University as a ground truth (see the web site at http://www.bic.mni.mcgill.ca/brainweb). The first aspect is the image information represented by the principal components during feature extraction. The second one is the properties of the self-adaptive algorithm, including discriminatory ability, stability, and sensitivity to the initial parameters. The third one is the quantitative evaluation of the segmentation, including accuracy, efficiency, and robustness against noise.

2. METHOD

In this section, we first discuss the clustering analysis method, which is a self-adaptive online vector quantization algorithm. Then its application to MR images is described in details.

2.1. Self-adaptive online vector quantization algorithm

The main idea of our method is to classify voxels based on their local intensity vectors rather than their own intensities only. For each voxel, we construct a local intensity vector, which contains that voxel and its neighbors.

2.1.1. Feature extraction

The constructed 3D volume data of vectors have a very large size and require intensive computing effort to process. To reduce the computing burden, we apply the PCA to the local intensity vector series of the MR image. The first few components, which sum up to 90% of the total variance, are chosen to optimize or minimize the dimension of the feature vectors. The corresponding K-L transformation matrix is generated from the MR image data. Then, the feature vector series are generated via the K-L transformation matrix from the local intensity vector series. Only the first few components will be retained for the feature space classification, and the remaining components with very little information will be ignored.

2.1.2. Classification of feature vectors

A self-adaptive online vector quantization algorithm [4] was modified to classify the feature vector series. This data-oriented algorithm is fully automated. The mathematical theory behind this algorithm is the central limit theorem [8].

Let $\{X_i \in \mathbf{R}^4 : i = 1, 2, 3, \ldots, N\}$ be the series of the feature vectors, where N is the dimension of feature vectors. Let K be the possible maximum class number and T be a threshold adaptive to the data set. Let $dist(\boldsymbol{x}, \boldsymbol{y})$ be the Euclidean distance between vectors $\boldsymbol{x}$ and $\boldsymbol{y}$. The algorithm scans from the first voxel to the last one in the image. In the beginning, there is only one class and its representative vector is the feature vector of the first voxel (initial condition.) For each next voxel, the Euclidean distance $dist(*, *)$ between its feature vector and the representative vectors of existed classes is calculated. If $dist(*, *) < T$, the representative vector of the current class is updated. If not, a new class will be generated subject to the constraint of the maximum class number K. After a scan, the representative vectors of all classes are generated. Then, feature vectors are assigned to a class according to the nearest neighbor rule [4,5]. Detailed investigation on the nearest neighbor rule and others is under progress [13].

The segmentation results will depend on two parameters *K* (maximum class number) and *T* (threshold). In our experiments, *K* is determined based on the anatomical knowledge, whereas the optimal value of *T* is set to the maximum component variance of the feature vector series.

2.2. Application to MR images

A 3D first-order Lagrange interpolation procedure [12] is first applied to the MR image data set for an adequate local intensity vector on each voxel. We choose a linear interpolation procedure in our implementation in order to preserve partial volume effects, which appear commonly in MR images. Nonlinear interpolation is not suitable in this application since it may change the distribution of partial volume effects. Other advantages of the interpolation can be observed that an interpolation actually performs as a low-pass filter. Therefore, the high-frequency noise can be minimized. In addition, an interpolation procedure increases the size of samples to ensure a stable estimation of the feature parameters.

In order to extract the region of brain volume and eliminate surrounding background and skull/scalp of the MR images, a rough segmentation is first performed on the interpolated data set. When the maximum number of classes *K* is set to 3, the self-adaptive online vector quantitation algorithm automatically identifies brain tissues and cerebrospinal fluid (CSF), skull/scalp, and outside background. A morphology dilation filter and region growing technique are applied to extract the brain volume region including CSF. Further segmentation is performed only in the extracted region.

The self-adaptive online vector quantization algorithm is now performed to the interpolated MR data set within the extracted region. For each voxel, a local intensity vector is formed by itself and its neighbor voxels in a sphere shape. For the simulated brain MR images with voxels of 1 mm cubic size, the window covering the neighbors consists of 19 voxels as shown in Figure 1. During feature analysis, 90 percent of the total variance is selected to optimize the dimension of the feature vectors. This results in a dimension size for the feature vectors to be 4 or 5, dramatically minimizing the computation burden and achieving high computing efficiency. During the feature analysis, a K-L transform matrix is generated, which is then used to transform the local intensity vector series to the feature vectors in the K-L domain.

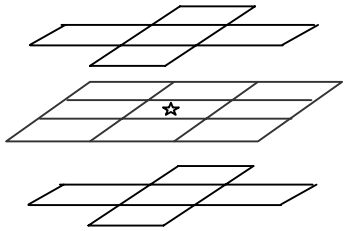

Figure 1: A description of local intensity vectors in three dimensions. The current voxel is marked by an asterisk.

Estimating the representatives of the feature vectors can be regarded as a learning procedure, which is a data-oriented automatic approach. The representative elements of each class are obtained by an online scan. We can label each feature vector to a class according to a nearest neighbor rule. After classification, the segmentation results follow an inverse interpolation procedure and are resized back to the original image size.

3. EVALUATION OF THE SELF-ADAPTIVE ONLINE VECTOR QUANTIZATION SCHEME

3.1. Evaluation of the feature extraction

During feature analysis, we choose the first 5 principal components, which sum up to, at least, 90% of the total variance, for minimizing the dimension of the feature vectors. Figure 2 shows the first 5 component images in the K-L domain with a decreasing order of significance. The purpose of the feature extraction is to retain the majority information of the images for reducing the computation burden, neglecting other components that carry very little information. It is clear that these first five components represent the dominant information. As we can see in the figure, the last (5^{th}) component reflects marginal information (partial volume effects) among classes. Those components beyond the 5^{th} one contain even much less information.

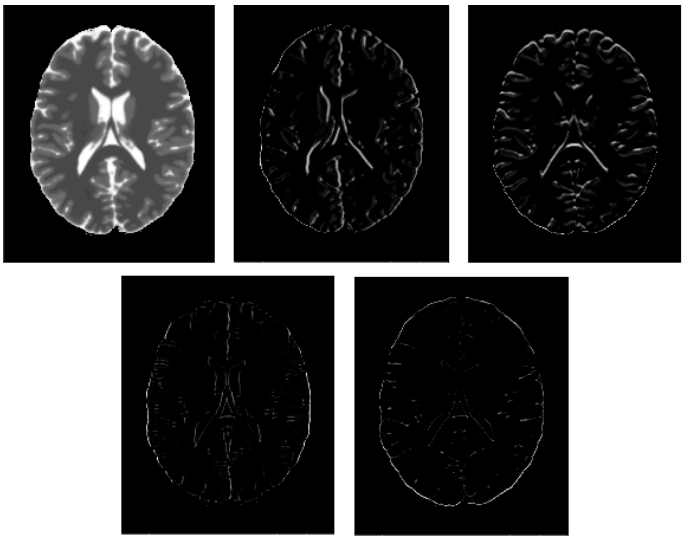

Figure 2: The component images in the K-L domain. On the top, components 1, 2, and 3 are shown from left to right. On the bottom, left one is component 4 and right one is component 5.

3.2. Evaluation of the self-adaptive online vector quantization

In this section, we apply the self-adaptive online vector quantization algorithm to the synthesized data to test the stability and discriminatory properties of our method described in Section 2. Similar to Markov Random Field models [14], MR image data can be well modeled as a finite Gaussian mixture distribution. Each vector has a multivariate Gaussian distribution with mean vector μ and covariance matrix ψ.

Let Y denote a p-variant random vector measured in K classes. The 3D volume data of MR images can be modeled with mixture density of

$$f_Y(y) = \sum_{j=1}^{K} \pi_j f_j(y) \tag{1}$$

$$f_j(y) = (2\pi)^{-p/2} (\det \psi_j)^{-1/2} \exp[-\frac{1}{2}(y-\mu_j)' \psi_j^{-1} (y-\mu_j)] \tag{2}$$

where π_j is a prior probability and $f_j(y)$ is the Gaussian distribution of the j-th group. This mixture model specifies the distribution of each data vector Y_j over the K classes with different weights $\{\pi_j\}$.

Initial Pixel Values	Estimated Parameters $\{\mu_1^*, \sigma_1^*, \pi_1^*\}$, $\{\mu_2^*, \sigma_2^*, \pi_2^*\}$, $\{\mu_3^*, \sigma_3^*, \pi_3^*\}$
875	{1191, 84, 0.39}, {1781, 250, 0.42}, {3490, 437, 0.19}
1326	{1205, 93, 0.40}, {1815, 238, 0.41}, {3505, 429, 0.19}
1550	{1205, 93, 0.40}, {1815, 238, 0.41}, {3505, 429, 0.19}
2858	{1205, 93, 0.40}, {1815, 238, 0.41}, {3506, 422, 0.19}
4186	{1206, 94, 0.40}, {1818, 244, 0.41}, {3509, 427, 0.19}

Table 1: Estimated model parameters with different initial values.

One-dimensional (p = 1) synthesized data were generated, where the parameters of various classes were obtained from the anatomical model in the Connell Brain Imaging Center database. The sample size was selected as 100x100x100. There are three tissue classes, white matter, gray matter, and cerebrospinal fluid (CSF), with true mean and standard deviation values μ_1 = 1191, σ_1 = 79, μ_2 = 1735, σ_2 = 284, and μ_3 = 3483, σ_3 = 448 respectively. The corresponding weights are π_1 = 0.35, π_2 = 0.46, and π_3 = 0.19.

3.2.1. Stability to the initial value

To test the stability property of our method, we performed an experiment with various initial values and estimate the representative parameters during learning procedure. Table 1 shows the estimated parameters with different initial values. It is indicated that our method is moderately independent of initial values with consistent estimated parameters for a large sample size 100x100x100. It is also noted that the classification rule for the results of Table 1 was the nearest neighbor rule, which may not be optimal, as seen by the weight estimation. Further investigations on optimal classification rules in terms of minimal error rate according to the highest posterior probability are then needed and are under investigation [13]. In addition, since we used 1-D synthesized data to simplify the tests on the segmentation scheme properties and furthermore the correlation among neighborhood voxels was not integrated during this test, more differentiation for the weight estimation is expected.

3.2.2. Discriminatory sensitivity

There are two dominant tissue mixtures in the brain MR images. One is the mixture of white matter and gray matter, which we call the white-gray mixture; the other is the mixture of gray matter and CSF, which we call gray-CSF mixture. Thus, our experiments were designed to test the discriminatory sensitivity of the method for these two dominant mixtures. Two Gaussian mixture distributions were generated based on these mixtures. The contrast-to-noise ratio (CNR) is defined by

$$CNR = \min\{\frac{|\mu_1 - \mu_2|}{\sigma_1}, \frac{|\mu_1 - \mu_2|}{\sigma_2}\} \tag{3}$$

where μ_1 and μ_2 are the true mean intensity levels of pixels in two adjacent regions. And the normalized root mean-square error (NRMSE) is defined by

$$NRMSE = \sqrt{\frac{(\mu_1 - \mu_1^*)^2 + (\mu_2 - \mu_2^*)^2}{\mu_1^{\,2} + \mu_2^{\,2}}} \tag{4}$$

where μ_1^* and μ_2^* are the estimated mean values.

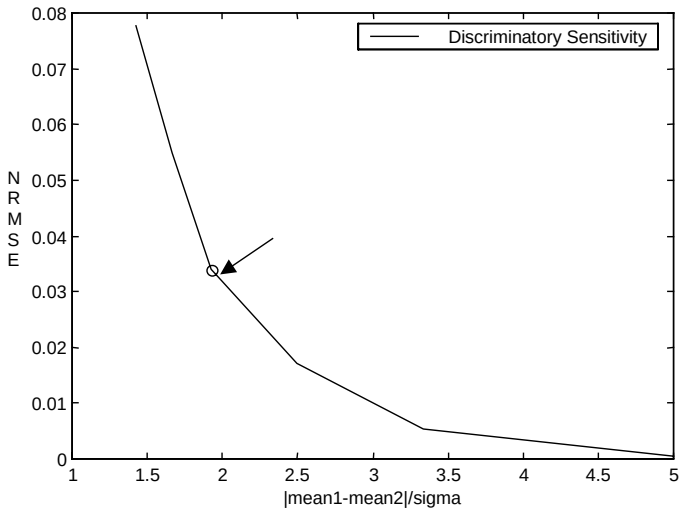

Figure 3: Discriminatory sensitivity tests of the NRMSE vs. CNR on the white-gray mixture with prior probability π_1 equivalent to 0.43 and π_2 equivalent to 0.57.

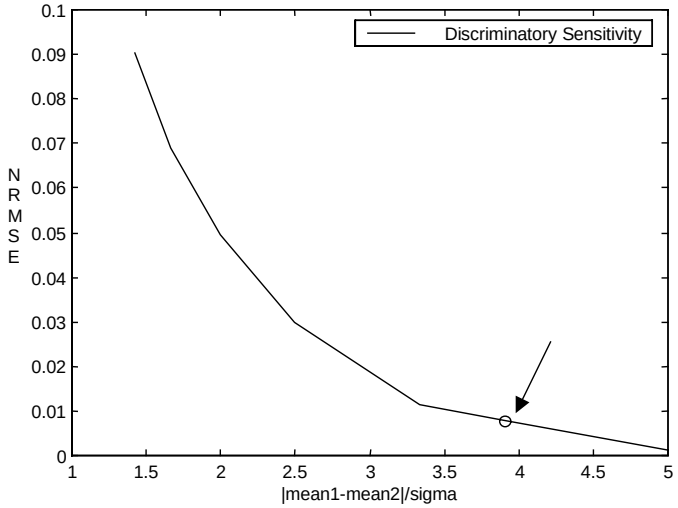

Figure 4: Discriminatory sensitivity tests of the NRMSE vs. CNR on the gray-CSF mixture with prior probability π_1 equivalent to 0.71 and π_2 equivalent to 0.29.

Figures 3 and 4 show the discriminatory sensitivity tests on the white-gray mixture and gray-CSF mixture respectively. The arrowed points indicate the corresponding CNR values in the anatomical model. The NRMSE values are 3.4% and 0.8% at that point respectively. These errors are very small, indicating an excellent discriminatory sensitivity.

4. EXPERIMENTAL RESULTS ON MR IMAGE DATA

4.1. MR data description

The performances of the above segmentation scheme were evaluated using the anatomical model in the Connell Brain Imaging Center of McGill University. In this study, the MRI phantom was simulated with T_2-weighted contrast and 1 mm cubic voxel size. The non-uniformity effect of image intensity was set to 0%.

A rough segmentation with class number equivalent to 3 was first performed on the data set in order to extract the ROI, eliminating the surrounding background of the MR image. It is necessary to extract the ROI because the existence of surrounding backgrounds would disturb the feature analysis. When the class number was set to 3, the algorithm segmented three regions: brain tissues including CSF, skull/scalp, and outside background. A morphology filter and region-growing technique were applied to extract the ROI of the brain volume. Figure 5(a) depicts a slice of the T_2-weighted MR image assuming 0% noise. Figure 5(b) shows the anatomical truth model of normal brain. The extracted ROI is shown in Figure 5(c).

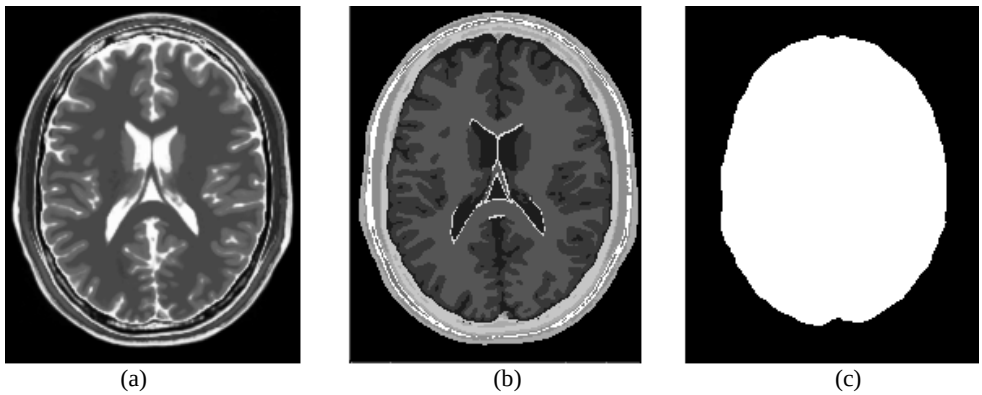

(a) (b) (c)

Figure 5: (a) one slice of a T_2-weighted MR image of 181x217 size, (b) the anatomical truth model, and (c) the extracted ROI.

4.2. Evaluation of MR image segmentation

Figure 6 shows the three classes segmented from the MR image of Figure 5(a): white matter, gray matter, and cerebrospinal fluid (CSF), with our segmentation scheme. A quantitative evaluation of the algorithm by the misclassification rate of the segmentation is shown in Table 2. The misclassification rate is defined as the ratio between the number of pixels misclassified by the algorithm and the total number of pixels in the dataset.

(a) (b) (c)

Figure 6: The three classes segmented from the MR image, (a) white matter, (b) gray matter, and (c) CSF.

4.3. Robustness against noise

We also tested the robustness of the algorithm against noise. In the experiments, two noise levels of 1%, and 3% were added to the phantom image of Figure 5(a) respectively. The noise level indicates the percentage noise added to the base signal. Table 2 shows the misclassification rates at different noise levels. It is clear that the less the noise, the small the misclassification rate. In a certain range of noise levels, say less than 3%, our algorithm demonstrates a robustness property against noise.

Noise Level	0%	1%	3%
Misclassification rate	4.19%	4.52%	5.95%

Table 2: Overall misclassification rates in the brain MR image segmentation with different noise.

4.4. Computing efficiency

The principal component analysis method reduces significantly the computation burden. For 50 image slices of 256x256 array size, the computing time for the segmentation took only 30 seconds on a PC/Pentium II with 300 MHz CPU and 512 MB memory space. The computing efficiency has been tremendously improved, as compared with those methods based on Markov Random Field models [14].

5. DISCUSSION AND CONCLUSIONS

The general goal of our approach is to develop a fast and self-adaptive algorithm for MR image segmentation. This approach is a valuable strategy in practice. From the presented experimental results, it can be seen that our method has a number of advantages in (1) computing efficiency, (2) moderate stability to the initial values, (3) accuracy, and (4) robustness against noise.

During feature classification, there are two input parameters that need to be pre-determined. One is the total class number K, and the other is the threshold T for generating a new class. In our experiments, the value of K is chosen based on anatomical knowledge, i.e., the total possible tissue numbers plus partial volume induced classes. An optimal value of T is empirically set to the maximum component variance of the feature vector series. This choice selects the least number of classes with

maximal differentiated features. We have verified the optimal value of *T* empirically based on the ground truth of simulated MRI phantom with several noise levels. Further work on theoretical analysis of the optimal *T* is still needed.

In the application to MR image segmentation, our method considers not only the voxel intensities and their neighbors, but also the anatomical knowledge of the MR images. This approach utilizes *a priori* anatomical knowledge to extract the ROI. The data-oriented classification algorithm does not depend on the initializations. The classification demonstrated efficient and robust performances. The fast and self-adaptive properties of this algorithm make it valuable and practical for other applications in medical image segmentation. The feasibility of this approach to study MR images of larynx is demonstrated in [5].

ACKNOWLEDGEMENTS

This work was supported in part by a NIH Grant #CA79180 and a fund from Viatronix Inc. and MD OnLine Inc. The authors wish to thank Dr. Ing-Tsung Hsiao for valuable discussions.

REFERENCES

1. M. Bomans, K. H. Hohne, U. Tiede, and M. Riemer, "Three-dimensional segmentation of MR images of the head for 3D display", *IEEE Trans. Medical Imaging*, **9**: 177-183, 1990.
2. M. E. Brandt, T. P. Bohan, L.A. Kramer, and J. M. Fletcher, "Estimation of CSF, white and gray matter volumes in hydrocephalic children using fuzzy clustering of MR images", *Comput. Med. Imaging Graph*, **18**: 25-34, 1994.
3. M. A. Brown, and R. C. Semelka, *MRI basic principals and applications*, chapter 4, Wiley-Liss, New York, 1995.
4. D. Chen, L. Li, and Z. Liang, "A self-adaptive vector quantization algorithm for MR image segmentation", *7th ISMRM*, **1**: 122, 1999.
5. D. Chen, B. Li, P. Roche, W. Huang, and Z. Liang, "Virtual laryngoscopy: feasibility studies by CT and MRI", *Conf Record IEEE NSS-MIC*, **3**: 1583-7, 1999.
6. L. P. Clarke, R. P. Velthuizen, S. Phuphanish, J. D. Schellenberg, J. A. Arrington, and M. Silbiger, "MRI: stability of three supervised segmentation techniques", *Magn. Reson. Imaging*, **11**: 95-106, 1993.
7. L. P. Clarke, R. P. Velthuizen, M. A. Camacho, J. J. Heine, M. Vaidyanathan, L. O. Hall, R. W. Thatcher, and M. L. Silbiger, "MRI segmentation: methods and applications", *Magn. Reson. Imaging*, **13**: 343-368, 1995.
8. W. Feller, *An introduction to probability theory and its applications*, 3rd edition, John Wiley & Sons, 1968.
9. G. Gerig, J. Martin, R. Kikinis, O. Kubler, M. Shenton, and F. A. Jolesz, "Unsupervised tissue type segmentation of 3D dual-echo MR head data", *Image Vision Comput*, **10**: 349-360, 1992.
10. A. Gersho, and R. M. Gray, *Vector quantization and signal compression*, Klumer Academic Publishers, 1992.
11. L. O. Hall, A. M. Bensaid, L. P. Clarke, R. P. Velthuizen, M. S. Silbiger, and J. C. Bezdek, "A comparison of neural network and fuzzy clustering techniques in segmenting magnetic resonance images of the brain", *IEEE Trans. Neural Networks*, **3**: 367-682, 1992.
12. A. K. Jian, *Fundamentals of digital image processing*, Prentice Hall, Englewood Cliffs, NJ, 1989.
13. L. Li, D. Chen, H. Lu, and Z. Liang, "Comparison of quadratic and linear discriminant analyses in self-adaptive feature vector quantization scheme for MR image segmentation", submitted to *ISMRM*, 2001.
14. Z. Liang, J. R. MacFall, and D. P. Harrington, "Parameter estimation and tissue segmentation from multispectral MR images", *IEEE Trans. Medical Imaging*, **13**: 441-449, 1994.
15. M. Ozkan, B. M. Dawant, and R. J. Maciunas, "Neural-network-based segmentation of multi-modal medical images: a comparative and prospective study", *IEEE Trans. Med. Imaging*, **12**: 534-544, 1993.
16. S. R. Raya, "Low-level segmentation of 3D MR brain images- a role-based system," *IEEE Trans. Medical Imaging*, **9**: 327-337, 1990.
17. M. S. Atkins, and B. T. Mackiewich, "Fully automatic segmentation of the brain in MRI", *IEEE Trans. Medical Imaging*, **17**: 98-107, 1998.